Journal of Applied and Natural Science
17(2), 810 - 820 (2025)
ISSN : 0974-9411 (Print), 2231-5209 (Online)
journals.ansfoundation.org

Research Article

Bioactivity of the amikacin: Selenium nanoparticles stabilized by chitosan (AK: CS-SeNPs) on *Proteus mirabilis* biofilm

Dalal M. Ridha*
Department of Biology, College of Science, University of Babylon, Iraq
Hawraa M.AL-rafyaia
Department of Biology, College of Science, University of Babylon, Iraq
Zahraa M. AL-Taee
Department of Biology, College of Science, University of Babylon, Iraq

*Corresponding author. E-mail: sci.dalal.showali@uobabylon.edu.iq

Article Info
https://doi.org/10.31018/jans.v17i2.6563
Received: January 04, 2025
Revised: June 01, 2025
Accepted: June 05, 2025

How to Cite
Ridha, D. M. *et al.* (2025). Bioactivity of the amikacin: Selenium nanoparticles stabilized by chitosan (AK: CS-SeNPs) on *Proteus mirabilis* biofilm. *Journal of Applied and Natural Science*, 17(2), 810 - 820. https://doi.org/10.31018/jans.v17i2.6563

Abstract
Biofilm-associated diseases have become a challenging issue for the healthcare system due to the aggregation of bacteria within the biofilm, which exhibits increased resistance to broad-spectrum antibiotics at standard or elevated concentrations. Consequently, adopting Chitosan-stabilized selenium nanoparticles (CS-SeNPs) is an efficient way to regulate biofilm creation. Multiple analyses were applied to characterize CS-SeNPs, including ultraviolet-visible absorption, Fourier Transform Infrared Spectroscopy, Zeta potential analysis, Dynamic Light Scattering analysis, Field emission Scanning Electron Microscopy, and Energy Dispersive x-ray. The antibacterial and antibiofilm properties of CS-SeNPs, AK: Cs-SeNPs, and amikacin (AK) were tested using 96-microtiter plates. The resulting data have revealed that CS-SeNPs at a wavelength of 244 nm were stabilized and rounded in shape with an average size of 68±23nm. The minimum inhibitory doses of AK and CS-SeNPs required to prevent the growth of *P. mirabilis* were 1000±398 and 50±0 µg/mL, respectively. The combination of AK:CS-SeNPs inhibited *P. mirabilis* strains at MIC of 160±0:12.5±0 µg/mL, which is lower than the MIC of AK and CS-SeNPs applied alone. The lowest concentrations of AK:CS-SeNPs, ranging between 66±23:5±1 µg /mL and 93±23:8±3 µg /Ml, successfully impeded the initial creation of *P.mirabilis* biofilm .The results demonstrate that The conjugation of AK:CS-SeNPs improves the amikacin's bactericidal efficiency, significantly hinders biofilm's initial development and reduces the viability of established biofilm created by multidrug-resistant *P.mirabilis*. This therapeutic approach has the potential to serve as a promising strategy for addressing Biofilm-associated diseases caused by resistant strains of *P.mirabilis*, conferring confidence in the battle against persistent infections.

Keywords: Antibacterial impact, Antibiofilm impact, Amikacin, Chitosan, Mature biofilm, *Proteus mirabilis*, Selenium nanoparticles

INTRODUCTION

Proteus mirabilis is recognized as an enteric, gram-negative, rod-shaped bacterium in the class Gamma proteo-bacteria. It has recently been categorized as a genus within the order Enterobacteriales, family Morganellaceae. It is an agent that induces biofilm creation by assimilating surface organelles, including fimbriae and other adhesions, on the surface of inserted urinary catheters (Armbruster *et al*., 2018). The primary cause of urinary tract infections is supposed to be *P.mirabilis*, which is transmitted from the gastrointestinal tract or through direct contact (Schaffer and Pearson, 2016). Urinary tract infections (UTIs), which occur in the presence of catheters, are among the most prevalent nosocomial infections, accounting for about 40% of infections in healthcare institutions and representing 80% of all UTI (Jacobsen *et al.,* 2008). Infection with antibiotic-resistant pathogens remains a considerable concern and a substantial burden on the healthcare system in the United States and globally (Fang *et al.,* 2020).

Recent studies by Jernigan and colleagues have shown a decline in infection rates of antibiotic-resistant pathogens such as methicillin-resistant *Staphylococcus aureus* (MRSA), vancomycin-resistant *Enterococcus* (VRE), multidrug-resistance *Pseudomonas aeruginosa*, carbapenem-resistant *Acinetobacter* (Jernigan *et al*., 2020). This reduction in infection rates results from

implementing a new approach to address multidrug resistance pathogens involving vaccines, probiotics, bacteriophages, and monoclonal antibodies (Fang *et al.,* 2020). It has been found that *E. coli*, *K. pneumonia*, *Salmonella spp., Shigella spp., N. gonorrhoeae, Acinetobacter spp., S. aureus*, and *S. pneumoniae* are the eight pathogens that are most likely to spread in a health care institution. The proliferation of these pathogens also indicates the emergence of antibiotic resistance (World Health Organization, 2017). Superbugs are bacteria that have become resistant to several antibiotics. Superbugs can avoid the action of antibiotics by acquiring genes that immunize them from other pathogens (Medina *et al.,* 2016). Nanoscience is a scientific discipline focused on the object in the form of nanoscale. Various types of metal nanoparticles, including copper, silver, gold, iron, titanium and, selenium, etc., have been extensively researched for their biological applications, such as anticancer, antifungal, and antimicrobial activities in the medical field, owing to the unique characteristic of metallic nanoparticles having a large surface to volume ratio (Roy *et al.,* 2025). Metal materials in nanosized measure demonstrate distinctive physical properties that differ from their ions and bulk counterparts. This feature enables the nanoparticle to penetrate microbial cells and inflict molecular damage (Morones *et al.,* 2005). The synthesis of nanoparticles in various dimensions and shapes is associated with adopting biological, chemical and physical approaches (Ridha *et al.,* 2021).

Nanoselenium can induce reactive oxygen species such as hydrogen peroxide (H2O2) and superoxide (O2−), placing it at the forefront of biomedical applications. Renowned for its potent antibacterial and anticancer properties, selenium remarkably proves essential for improving health care (Geoffrion *et al.,* 2020). Selenium is a vital micronutrient that safeguards the body from oxidative damage and improves immunological function. Nanosized selenium has recently attracted considerable interest from researchers because of its remarkable biological features. Due to its potent antioxidant capabilities, proficiency in removing pollutants, and remarkable thermal stability, nanosized selenium presents promising benefits that could revolutionize our health and wellness strategies (San Keskin *et al.,* 2020). The study investigates the bioactivity of amikacin selenium nanoparticles coated with chitosan (AK:CS-SeNPs) regarding their influence on the biofilm creation of *P. mirabilis.*

MATERIALS AND METHODS

Preparation and analysis of selenium nanoparticles

Following a chemical reduction method, stabilized selenium was prepared using sodium selenite Na_2SeO_3 (precursor salt), chitosan (stabilizing factor), and ascorbic acid (reducing factor), as shown below. Firstly, chitosan (0.1g) was dissolved in 100 mL of 1% acetic acid to prepare this solution. The second step involved transferring 7.5 ml of ascorbic acid with a concentration of 0.51M to a flask containing 15 mL of chitosan solution. Then, 1mL of sodium selenite solution (0.51M) was carefully added along the flask walls. The flask was then placed on a shaker for 15 minutes until the solution turned red. Finally, the volume was filled up to 30 ml using deionized water to obtain the required 500 µg/mL concentration. Using the same procedure for synthesizing CS-SeNps, amikacin (0.077 g) was added to 1 mL of sodium selenite (0.51M) to prepare the conjugation Ak:CS-SeNps. The conversion of the solution color to red indicates the production CS-SeNPs and AK:CS-SeNPs. The red solution containing (CS-SeNPs, AK:CS-SeNPs) was subjected three washes with deionized water using a cooling centrifuge at 1200 RCF for 10 min to separate the generated CS-SeNPs, AK:CS-SeNPs. After collecting the precipitation, deionized water was added and subsequently transferred into a container covered with aluminium foil. The rinsed nanoparticles were stored at 4C for further procedures. To characterize the obtained CS-SeNPs, physical and chemical properties were studied using various techniques, including ultraviolet-visible absorption (UV-Vis), Fourier Transform Infrared Spectroscopy (FT-IR), Zeta potential analysis, Dynamic Light Scattering analysis (DLS), Field emission Scanning Electron Microscopy (FE-SEM), and Energy Dispersive x-ray (EDX).

Samples collection

The eight clinical samples of *P. mirabilis* were received from the frozen glycerol cultures of the Department of Biological Science, Babylon University. Bacterial isolates were cultured in Brain heart infusion broth (BHIB; HI Media, India) and kept at 37 °C for 24 h.

Proteus mirabilis isolates susceptibility towards antibiotics

The Kirby-Baure method was applied to screen the susceptibility of eight clinical samples of *P. mirabilis* toward various antibiotics, including amikacin (AK) 30µg; tobramycin (TOB) 10µg; aztreonam (ATM) 30µg; ceftazidime (CAZ) 30µg; cefotaxime (CTX) 30µg; cefepime (FEP) 30µg; ciprofloxacin (CIP) 10µg; nalidixic acid (NA) 30µg; ofloxacin (OF) 5µg; ertapenem (EIP) 10µg; trimethoprim (TMP) 5µg. At first, the turbidity of 0.5 McFarland fresh for bacterial suspensions was prepared, and the amount of the suspensions with swabs was spread at the surface of Muller-Hinton agar (MHA) plates. After inoculation, six antibiotic discs were arranged on the cultured petri dishes and brooded at 37 ºC for one day. The inhibition area observed surrounding each disc was documented. The response of clinical samples to antibiotics was assessed by measuring

the widths of the inhibition zones and comparing them with standard values remembered in the guideline M100 of CLSI 2024.

Estimation of the bacterial impact of the combination AK: CS-SeNPs upon *Proteus mirabilis* samples

Following the CLSI 2020 guideline M07 105, the 96-well microplate method was performed to detect MIC of CS-SeNPs, AK:CS-SeNPs, and AK towards *P. mirabilis* samples. Initially, overnight cultures of *P. mirabilis* samples cultivated in Brian heart infusion broth (BHIB) were diluted to obtain the concentration of 0.5 MacFarland (1.5×10^8 CFU/m). A series of twofold dilutions of CS-SeNPs, AK:CS-SeNPs, and AK was conducted using 50 µL of Muller Hinton broth (MHB). The concentrations of SeNPs alone varied from 400 to 0.4 µg/mL, for AK:CS-SeNPs from 1280:100 to 2.5:0.2 µg/ml, and for AK alone from 2560 to 2.5 µg/mL. A volume of 50 µL of inoculated MHB for each tested sample with concentration 1×10^6 CFU / mL was dispersed into the well of microtiter plates. The cultured microtiter plates were placed in an incubator for one day at 37◦C. Following the incubation time, the MIC was recorded as the lowest concentration of the treatment substance, which did not exhibit apparent bacterial turbidity. Meanwhile, minimum bactericidal concentration (MBC) is established as the most miniature treatment necessary to achieve a 99.9% reduction of the treated bacteria. The MBC was determined by culturing a volume of 10 µL of each well with a transparent appearance on the Brian heart infusion agar (BHIB) plates and kept at 37◦C for 24 hours.

Determination of the anti-biofilm effect of AK: CS-SeNPs at the early stage of *Proteus mirabilis* biofilm creation

The antibiofilm effect of CS-SeNPs, AK:CS-SeNPs, and AK were tested at the early stage of biofilm generation upon four isolates of *P. mirabilis*, which were the strongest biofilm formers according to the Congo red method (Kaiser *et al.,* 2013). Firstly, the flat bottom 96 microplates were used to make the two serial MIC concentrations of CS-SeNPs, AK:CS-SeNPs and AK, performed in the wells of microplates containing 100 µL sterilized distal water. The fresh broth of *P. mirabilis* isolates at 0.5 McFarland was carefully adjusted to reach 1×10^6 CFU/ml bacterial growth. It was accomplished by adding a double concentration of tryptic soy broth enriched with 2% sucrose, ensuring an ideal environment for robust growth. A 100 µL inoculation of each bacterial isolate was transferred to the well of the microplate containing a diluted concentration of tested compounds separately. The edges of cultured microplates were covered with parafilm and kept in an incubator for two days at 37 ◦C. After 48 hours, the solutions in microplate wells were gently aspirated and rinsed with phosphate buffer to remove cells that were not attached to the microplate wells. After drying the inoculated microplates containing the biofilm, 200 µL of Ethanol was distributed and remained for 15 minutes to fix the adherent biofilms. After removing Ethanol, 200 µL of 1% crystal violet stain was added to the well of microplates. After 20 minutes, the stained microplates were washed carefully with tape water to release the unattached stains. After drying, 200 µL acetic acid was transferred to the microplate wells and mixed well to release all adherent stains. A microplate reader plate (BioTek-ELX800) at 490 nm is used to measure the quantity of adherent biofilm. The minimum biofilm inhibition concentration (MBIC) of (CS-SeNPs, AK: CS-SeNPs, and AK) was the lowest dose, eradicating 90% of bacterial cells to generate biofilm. The ratio of MBIC was recorded as below (Bardbari *et al*., 2018) :

$$\mathrm{MBIC} = \left[1 - \left(\frac{\text{Treated well absorbance}}{\text{Control well absorbance}}\right)\right] \times 100 \qquad \text{Eq. 1}$$

Impact AK:CS-SeNPs on the biofilm viability of *Proteus mirabilis* and detection of their half maximal inhibitory concentration (IC_{50})

The 3-[4,5-dimethylthiazol-2-yl]-2,5-diphenyltetrazolium bromide (MTT) technique was employed to assess the impact of Cs:SeNPs, AK-Cs:SeNPs, and AK on the availability of *P.mirabilis* biofilms (Karthik *et al.,* 2024). The MTT assay quantifies the amount of insoluble purple formazan granules generated by the reduction of yellow tetrazole by the electron chain respiratory system found in active cells (Lin *et al.,* 2021). Determining the impact of the tested compound on the mature biofilm required adjusting the tensity of fresh broth of *P.mirabilis* isolates at 0.5 McFarland to reach bacterial growth 1×10^6 CFU/ml by addition of tryptic soy broth containing sucrose (2%). A 200 µL inoculations of each bacterial isolate were transferred separately to the well of the flat bottom 96 microplate. The edges of cultured microplates were covered with parafilm and kept in an incubator for two days at 37 ◦C. After 48h, the solutions in the microplate wells were discarded carefully and washed with phosphate buffer to expel non-detached cells. To obtain the two-fold dilution of the tested compounds, a volume of each solution (CS-SeNPs, AK:CS-SeNPs, and AK) was diluted in eppendorf tubes to get the required concentrations. A after that, a volume of 200 µL of serial twofold dilutions were transferred into wells. The treated flat bottom 96 microplates flat bottom 96 microplates were kept in incubator for one day at 37 ◦C. Estimation a viability of biofilm, exposed to different concentrations of tested compound, was carried by transferring 200 µL of MTT dye which prepared by dissolving 0.5 mg of MTT in 1mL of PBS, into each well of microtiter plates. The stained microplates were placed in incubator at 37 °C for one hour. The formazan crystals assembled by the biofilm's active bacteria

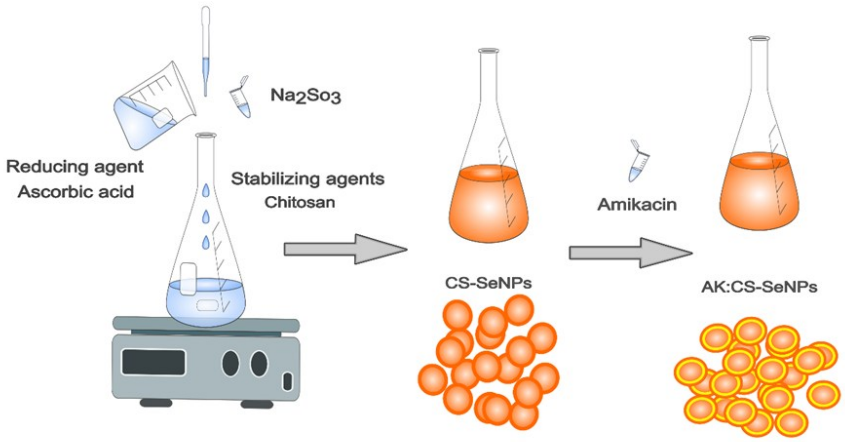

Fig. 1. *Schematic representation of the chemical preparation of selenium nanoparticles (CS-SeNPs) utilising sodium selenite (Na2SeO3) as precursor salt which is reduced by ascorbic and subsequently coated with stabilizing agent (chitosan) , followd by conjugation with amikacin (AK) to produce amikacin: selenium nanoparticles (AK: CS-SeNPs)*

were solubilized by adding dimethyl sulfoxide (DMSO) (200 µL) to the well of microplates. The plates were placed for 20 minutes at room temperature in the dark. The intensity of dissolved formazan was determined using an ELISA reader at 490 nm. A higher absorbance indicates an increased formazan concentration, suggesting a greater metabolic process within the bacterial biofilm. The ratio of biofilm activity was evaluated according to the following formula:

$$\% \text{ Biofilm activity} = \left(\frac{\text{An absorbance of tested well}}{\text{Absorbance of control well}}\right) \times 100$$

Eq. 2

Statistical analysis

The experiences were conducted three times; the resulting values were recorded as the mean ± standard deviation. The variance between the results was calculated by applying a one-way ANOVA analysis using the GraphPad Prism Software.

RESULTS AND DISCUSSION

Preparation and analysis of stabilized amikacin: selenium nanoparticles

Initially, selenium nanoparticles coupled with amikacin were carried out by reducing selenite ions by adding ascorbic acid to a solution containing green capping agents Chitosan (CS). As demonstrated in (Fig. 1), the formation of CS-SeNPs and AK:CS-SeNPs was verified by the solution's color transition from colorless to reddish brick. A stabilizing agent (Chitosan) is applied in synthesizing selenium nanoparticles, conferring the surface of selenium nanoparticles (CS-SeNPs) positive charges that modulate adhesion and interaction on the surface of microbial membranes. This interaction creates intracellular free radicals derived from oxygen molecules, impeding microbial bioactivity and enhancing cell membrane permeability (Karthik *et al.,* 2024). The pH fluctuation and enzymatic treatment do not influence the selenium nanoparticles coated by chitosan. It is also easily liberated from chitosan due to exposure to free radicals (Zhang *et al.,* 2015).The particle size of CS-SeNPs is attributed to the intensity of the color of the suspension of selenium nanoparticles, which is demonstrated as the maximum absorption of ultraviolet or visible light. On the other hand, the maximum absorption in the UV-Vis spectrum is directly proportional to the dimensions of selenium nanoparticles (Sentkowska and Pyrzyńska, 2022). The UV-Vis spectrum for CS-SeNPs and AK: CS-SeNPs was scanned from 180 to 300 nm, showing distinct absorption peaks at 244 nm, as illustrated in (Fig. 2A). The functional groups extended on the surface of selenium nanoparticles coated by chitosan were effectively analyzed using the FT-IR technique.

As observed in (Fig.2B), the CS-SeNPs' spectra reveal seven prominent peaks in the FT-IR spectrum scanned from 400 cm^{-1} to 4000 cm^{-1}. It confirms the successful stabilization and characterization of Selenium nanoparticles. According to the FT-IR spectra of CS and CS-SeNPs reported by Chen et al., several prominent peaks, including the vibrations of O-H at 3425.26, C-H at 2876.72, N-H at 1597.81, C-N at 1079.27, C-O at 285 were confirmed the recent CS-SeNPs FT-IR spectrum (Chen *et al.,* 2015). As exhibited in the AK: CS-SeNPs spectrum, six prominent peaks matched some peaks found in the CS-SeNPs spectrum and AK spectrum. The existence of a broad peak at 3414.93 cm−1 related to the O-H bond, the stretching group of (C-H) at 2939.52 cm^{-1} attributed to aliphatic chains of fatty-acid residues, and the weak vibration of the C=O band at 1629.35 cm^{-1} related to ester. As Figure(2B) shows, stabilized SeNPs exhibit stretching peaks from 1500 cm^{-1} to 1150 cm^{-1}, representing the stretching vibration

of –OH, while the beak at 1408 cm^{-1} belongs to the bending vibration of C-O (Wadhwani *et al.,* 2017). The prominent stretching vibrations for CS-SeNPs and AK: CS-SeNPs, observed at 705 cm^{-1} and 585 cm^{-1}, clearly indicate the binding of Se to –OH group as Se-O, establishing a definitive connection between ascorbic acid and selenium (Al Jahdaly *et al.,* 2021). The color intensity of colloidal SeNPs distinctly ranges from light to dark red, depending on the size of the nanoparticles. The color intensity of colloidal SeNPs distinctly ranges from light to dark red, depending on the size of the nanoparticles. As The volume of SeNPs increases, the red intensity becomes darker (Huang *et al.,* 2019).

The FE-SEM image in Fig.3 (B) at 200 nm displayed selenium nanoparticles stabilized by Chitosan (CS-SeNPs), which were uniformly dispersed , and spherical with an average size of 68±23nm. The antibacterial strategies dependent on the dimensions of employed selenium nanoparticles encompass the formation of reactive oxygen species (ROS), depletion of internal ATP, and disruption of plasma membrane ,leading to the release of proteins, polysaccharides, and other substances (Huang *et al.,* 2019). Furthermore, DNA damage and disruption of trans-membrane electron transport are critical mechanisms through which selenium nanoparticles (SeNPs) exhibit their antibacterial efficacy (Zhang *et al.,* 2021). The chemical structure of stabilized selenium nanoparticles was determined by applying EDX analysis, as shown in (Fig 3D). A selenium atom in the EDX spectra of CS-SeNPs confirmed the creation of selenium nanoparticles. The additional peaks like oxygen, carbon, nitrogen, and sodium observed in the spectra of CS-SeNPs are attributed to the capping agents utilized in the preparation. In addition, the DLS anaelysis exhibited the accurate hydrodynamic volume and distribution size of the stabilized selenium nanoparticles. The PDI value represents nanoparticle distribution size in liquid samples (Sharma *et al.,* 2014). Depending on the values of the polydispersity index PDI, the distribution size of nanoparticles is determined as monodispersed when the PDI value is less than <0.05, low polydispersity when the PDI value is less than <0.08, moderate polydispersity when the PDI value extended between 0.08 to 0.7, and broad polydispersity when the PDI value greater than 0.7 (Pachouri *et al.,* 2021). The hydro-diameter of CS-SeNPs was 302±151nm with a PDI of 0.188. The PDI value of CS-SeNPs is more significant than 0.08 and less than 0.7, which means the stabilized SeNPs have a moderate homogeneity in the size distribution. DLS is an intensity -based analysis that estimates the hydrodynamic radius of the scattered particles in liquid. At the same time, electron microscopy supplies the surface area depending on the intensity of the electron transmitted through the dried sample. Therefore, the volume acquired by DLS usually differs from the size of electron microscopy (Bhattacharjee, 2016). Chitosan is biodegradable organic compound that possesses the capability to promote electrical interaction between the surfaces of metal nanoparticles and biological membranes ,functioning as both a reducing and stabilizing agent (Javed *et al.,* 2022). The stabilized selenium nanoparticles were dispersed in pure water at 25C°as remembered in the zeta potential analysis; as observed in (Fig.4B), the surface charges of CS-SeNPs were equal to zero. However, the zeta potential values of SeNPs coated by the biocompatible capping agents (Chitosan) are equaled to 0 mV. The coated SeNPs were suspended and stabilized in the liquid state for more than three months at laboratory temperature. It was supposed that the zeta potential analysis could not determine the Brownian motion of SeNPs and detect the surface charge of stabilized nanoparticles due to the solubility of CS-SeNPs and the absence of the interface between the water and stabilized selenium nanoparticles (Yuan *et al.,* 2023).

Proteus mirabilis isolates susceptibility towards antibiotics

If a bacterial isolate shows resistance to one or more antibiotics across three distinct classes, it is considered multidrug-resistant (MDR) (Kamer *et al.,* 2024). This categorization is important for comprehending the diffi-

Table 1. Susceptibility of *Proteus mirabilis* samples over diverse classes of antibiotics

	Inhibition zone(mm)										
Sample Number	**AK 30µg**	**TOB 10µg**	**ATM 30µg**	**CAZ 30µg**	**CTX 30µg**	**FEP 30µg**	**CIP 10µg**	**NA 10µg**	**OF 5µg**	**EIP 10µg**	**TMP 5µg**
PM1	9 (R)	6 (R)	6 (R)	6 (R)	6 (S)	6 (S)	6 (R)	6(R)	16 (S)	11(R)	6 (R)
PM3	11(R)	23 (S)	11(R)	26(S)	12(S)	6 (S)	40(S)	21(S)	44 (S)	39 (S)	6 (R)
PM4	6 (R)	20 (S)	12(R)	6 (R)	6 (S)	6 (S)	30(S)	6(R)	34 (S)	26 (S)	8 (R)
PM5	6 (R)	19 (S)	12(R)	6 (R)	6 (S)	6 (S)	27(S)	6(R)	29 (S)	22 (S)	6 (R)
PM7	11 (R)	18 (S)	12(R)	6 (R)	6 (S)	6 (S)	30(S)	6 (R)	33 (S)	25 (S)	6 (R)
PM9	10 (R)	21 (S)	12(R)	6 (R)	6 (S)	6 (S)	34(S)	6 (R)	39 (S)	31 (S)	6 (R)
PM12	10 (R)	22 (S)	35(S)	25(S)	17 (S)	6 (S)	47(S)	24(S)	44(S)	38 (S)	27(S)
PM13	9 (R)	19 (S)	35(S)	17(R)	12 (S)	6 (S)	43(S)	24(S)	40 (S)	35 (S)	18 (S)

AK: amikacin; TOB: tobramycin; ATM: aztreonam; CAZ: ceftazidime; CAZ: cefotaxime; FEP: cefepime; CAZ: ciprofloxacin; NA: Nalidixic acid; OF: ofloxacin; EIP: ertapenem; TMP: trimethoprim

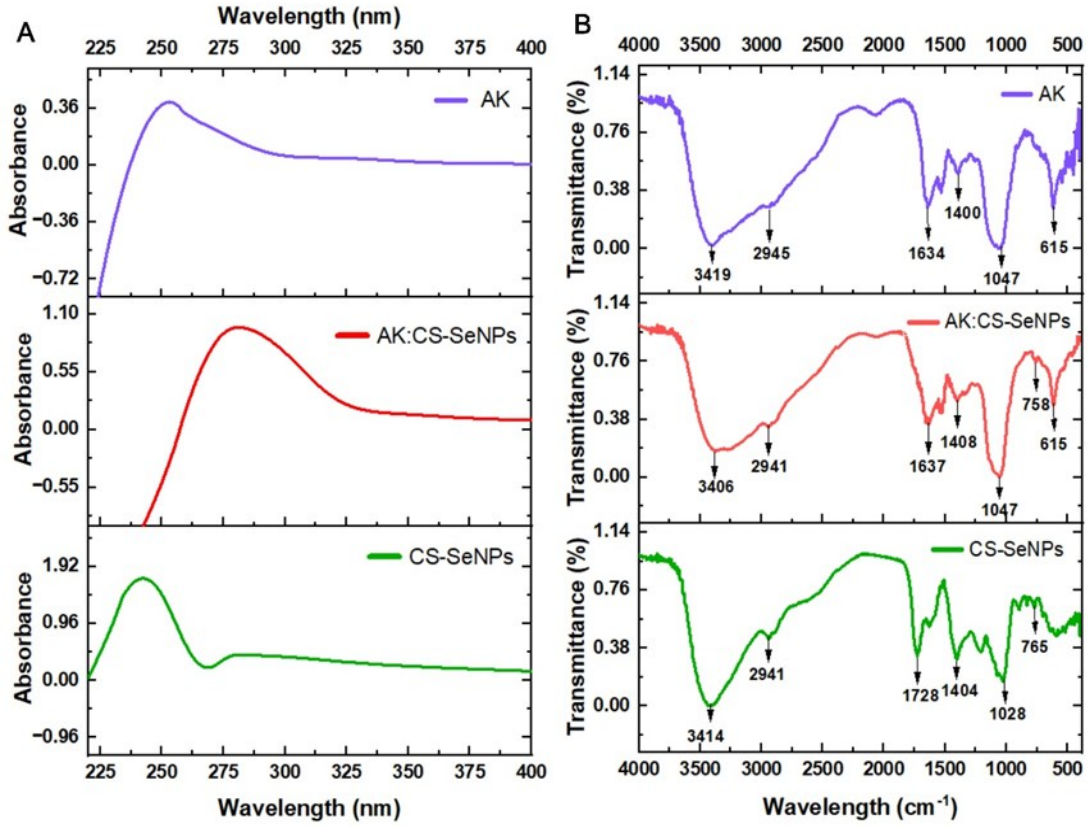

Fig. 2. *Description of selenium nanoparticles (CS-SeNPs), and a combination of Amikacin: selenium nanoparticles (AK: CS-SeNPs) prepared via a chemical technique using selenite salt as a precursor salt, ascorbic acid as a reducing agent and chitosan as a stabilizing agent. (A) UV spectra demonstrate peak absorption of CS-SeNPs at 245 nm and peak absorption of AK: CS-SeNPs at 275 nm. (B) FTIR spectra exhibit the existence of common functional groups of CS-SeNPs and AK in the spectra of AK: CS-SeNPs, confirming the binding of amikacin to the surface of CS-SeNPs*

culties in treating infections caused by these microorganisms. The multidrug resistance in *P.mirabilis* is attributed to integrons and several plasmids that confer tolerance to antibiotics belonging to the following classes: Penicillin, Cephalosporin, and Carbapenems through the transfer of the genes of extended-spectrum –lactamase (ESBLs), AmpC- type cephalosporinase, and AmpC- type carbapenemases (Tumbarello *et al.,* 2012).

The multidrug-resistant strains were identified by exposing *P.mirabilis* to multiple antibiotics associated with many classes. Reviewing the data in (Table 1), it is evident that all samples of *P. mirabilis* have a resistance to amikacin (AK). Furthermore, six samples resist aztreonam (ATM); however, only one resists tobramycin (TOB). Conversely, all strains were resistant to amikacin (AK), a member of the aminoglycoside class. All strains of *P. mirabilis* demonstrated sensitivity to cefotaxime (CTX) and cefepime (FEP). However, five strains demonstrated resistance to ceftazidime (CAZ), and the *P.mirabilis* samples (7 and 8) were susceptible to ciprofloxacin (CIP) and ofloxacin (OF), respectively. In contrast, five of the eight strains of *P. mirabilis* successfully overcome the antibacterial influence of nalidixic acid (NA) belonging to the quinolones and fluoroquinolones class. Seven out of *P. mirabilis* strains were targeted and devastated by ertapenem (EIP), part of the carbapenems class. Ultimately, it was found that six of the *P. mirabilis* strains were inhibited by trimethoprim (TMP), which is related to the folate pathway antagonist's class. As illustrated in Table (1), PM1, PM4, PM5, PM7, and PM9 were considered multidrug resistant.

Estimation of the bacterial impact of the combination AK: CS-SeNPs upon *Proteus mirabilis* samples

Enzymes associated with thiol, including thioredoxin and glutathione, are considered bactericidal agents distributed in Multidrug-resistant bacteria. In gram-negative bacteria, the silver nanoparticles conjugated with conventional antibiotics possess antibacterial efficacy by generating reactive oxygen species (RSO), which inhibits the thioredoxin enzyme and consumes glutathione (Zou *et al.,* 2018). The evolution of antibiotic-resistant bacteria among bacterial communities has been attributed to the excessive and improper administration of antibiotics. As a result, suitable metallic nanoparticles are used to augment conventional antibi-

Table 2. Detrimental effects of AK: CS-SeNPs on *Proteus mirabilis* samples

Tested agent	MIC(µg/mL)		MBC(µg/mL)	
	Range	Average ±SD	Range	Average ±SD
AK	320 -1280	1000±398[a]	640-1280	1120±296[a]
AK: CS-SeNPs	-	160±0[b]:12.5±0[d]	160:12.5-320:25	200±74[b]:15±5[d]
CS-SeNPs	-	50±0[c]	-	100±0[c]

CS-SeNPs: Chitosan-Selenium nanoparticles or AK: Amikacin representing its concentration in AK: CS- SeNPs. Small letters above each treatment associated with MIC or MBC concentration are significant at a P value less than or equal to 0.05.

Table 3. Efficacy of AK: CS-SeNPs upon the biofilm of *Proteus mirabilis* samples at an early stage

Bacterial sample	MBIC (µg/mL)		
	AK	AK: CS-SeNPs	CS-SeNPs
PM4	640±0[a]	66±23[b]:5±1[c]	20±7[c]
PM5	426±184[a]	80±0[b]:6±0[b]	20±7[b]
PM7	426±184[a]	66±23[b]:5±1[b]	41±14[b]
PM9	640±0[a]	93±23[b]:8±3[c]	20±7[c]

CS-SeNPs: Chitosan-Selenium nanoparticles or AK: Amikacin representing its concentration in AK:CS-SeNPs. Different letters above each bacterial sample associated with MBIC concentration for treatments are significant at a P. value less than or equal to 0.05.

otics (Kamer et al., 2024). After exposure of the eight samples of *P. mirabilis* to tested agents, AK: CS-SeNPs and CS-SeNPs, the lowest concentration of CS-SeNPs required to inhibit all *P. mirabilis* samples was 50 µg/mL, whereas the minimum inhibitory concentration of AK valued between 320 µg/mL to 1280 µg/mL. As observed in (Table 2), although inhibiting *P. mirabilis* samples, it has required high concentrations of AK compared to CS-SeNPs. The combination of AK: CS-SeNPs has an antibacterial impact on tested samples at low concentrations for both AK and CS-SeNPs (160±0:12.5±0). On the other hand, selenium nanoparticles enhance the antibacterial influence of amikacin to overcome *P.mirabilis* samples.

The MBC, responsible for decreasing the 3log bacterial growth of all *P.mirabilis* samples, was one concentration higher than the MIC value. In contrast, the average minimum concentration of AK to eradicate all tested samples was 1120±296 µg/mL. The data exhibited that the concentration of AK: CS-SeNPs at values between 160:12.5 µg/mL to 320:25 µg/mL inhibited *P.mirabilis* growth. Previous studies have exhibited that the antibiotics linked to silver nanoparticles can boost the attraction toward their targets, affect the penetrance of the cell membrane, and enhance the bactericidal impact of classical antibiotics. Both nanoparticles and antibiotics are powerful tools designed to eliminate bacteria through their distinctive bactericidal mechanisms. Therefore, conjugating two different bactericidal agents means killing the resistant pathogens in low concentrations (Haji *et al.,* 2022).

Determination of the anti-biofilm effect of AK: CS-SeNPs at the early stage of *Proteus mirabilis* biofilm creation

CS-SeNPs effectively develop reactive oxygen species (ROS), causing significant oxidative deterioration in pathogenic bacteria. Furthermore, the ROS produced by these nanoparticles influences the creation of bacterial biofilm (Huang *et al.,* 2016).

The formation of biofilm is a virulent factor that effectively enhances the ability of bacterial strains to resist the effects of various antibiotics. This experiment aims to estimate the antibiofilm impact of selenium nanoparticles linked with amikacin against different isolates of *P. mirabilis* forming biofilm. As exhibited in Table 3, the minimum concentration of AK necessary to inhibit the initial stage of producing biofilm ranged between 426±184 µg/mL and 640±0 µg/mL. The concentrations of CS-SeNPs necessary to inhibit biofilm information

Table 4. IC_{50} values and $MBEC_{60}$ values of AK, AK: CS-SeNPs, and CS-SeNPs exposed to the mature biofilm of *Proteus mirabilis* samples

Bacterial sample	IC_{50} (µg/mL)			$MBEC_{60}$(µg/mL)		
	AK	AK:CS-SeNPs	CS-SeNPs	AK	AK:CS-SeNPs	CS-SeNPs
PM4	1378±238[a]	268±46[b]:20±4[b]	225±38[b]	-	1280:100	-
PM5	1156±213[a]	427±26[b]:33±2[c]	190±29[bc]	-	1280:100	-
PM7	1155±277[a]	343±19[b]:26±1[b]	221±33[b]	-	640:50	-
PM9	1137±121[a]	379±42[b]:29±3[c]	227±28[b]	-	1280:100	-

CS-SeNPs: Chitosan-Selenium nanoparticles, AK: Amikacin. Different small letters above each IC_{50} for each bacterial sample are significant at p. value ≤ 0.05

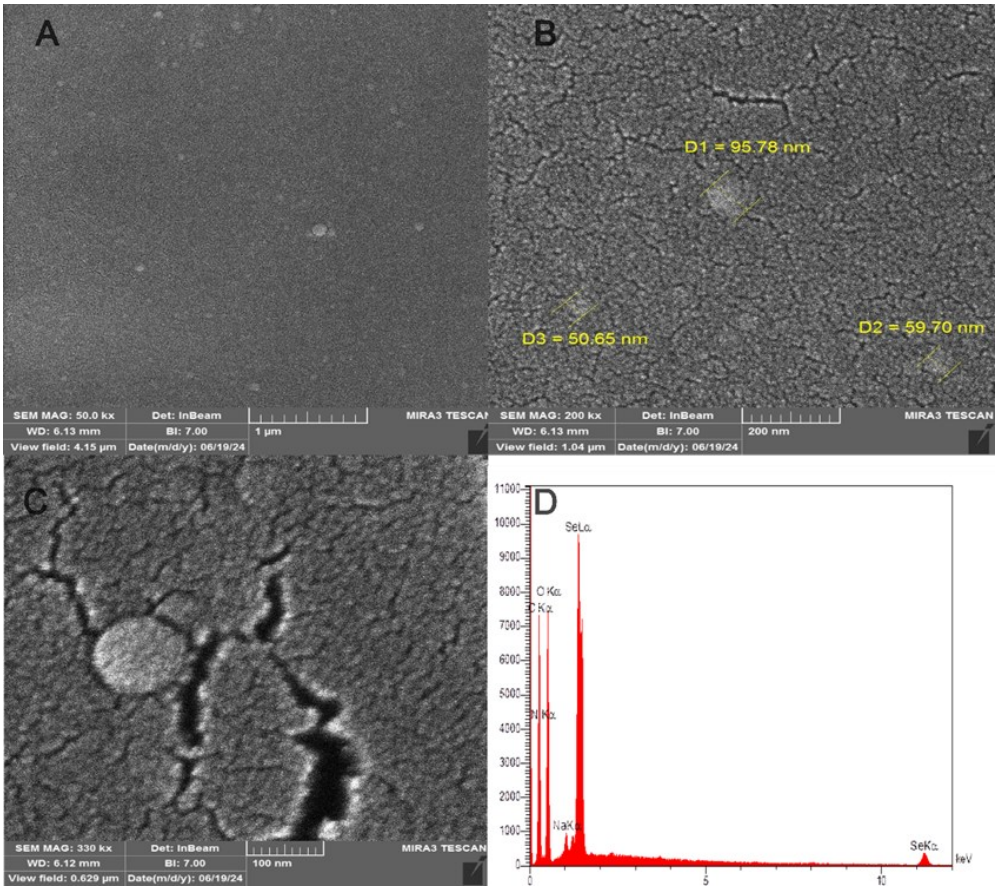

Fig. 3. *FE-SEM images exhibited that CS-SeNPs are evenly distributed and round with an average size of 68±23nm at various magnifications of (A) 1µm, (B) 200 nm and (C) 100 nm. (D) EDX spectra of CS-SeNPs indicated the presence of a selenium atom, validating the synthesis of selenium nanoparticles*

were 20±7 µg/mL for PM4, PM5, and PM9 and 41±14 µg/mL for PM7. In contrast, the concentrations of AK:CS-SeNPs were required to inhibit the biofilm creation of *P. mirabilis* samples at the early stage ranged between 66±23:5±1 µg/mL to 93±23:8±3 µg/mL. The comparison of the antibiofilm efficacy of SeNPs and AK used independently against *P. mirabilis* samples, in conjunction with Ak: CS-SeNPs, demonstrates that the synergistic effect of SeNPs allows for a reduction in the amikacin concentration, which is required to inhibit the biofilm of *P. mirabilis*. Shahmoradi and his colleagues demonstrated that selenium nanoparticles, measuring 77±27 nm, effectively reduced *E. faecalis* biofilm at 128 µg/mL and 64 µg/mL concentrations. Furthermore, their research confirmed that SeNPs combined with photodynamic therapy (PDT) significantly enhanced the reduction of the biofilm generation at 200 µg/mL and 400 µg/mL (Shahmoradi *et al.,* 2021).

Ak:CS-SeNPs impact on the biofilm viability of *Proteus mirabilis* and detection of their half maximal inhibitory concentration (IC_{50})

Nanoparticles coated with antibiotics were highly effective over gram-positive and gram-negative bacteria (Munir and Ahmad, 2022). A non- covalent combination (Gen:Bio-AgNPs) has augmented the spectrum activity of gentamicin over resistant *P. aeruginosa* stains in the presence of silver nanoparticles. High concentrations of AgNPs (400±112 µg/mL), GEN (1536±5 µg/mL) were reported to reduce the growth of tested strains. Conversely, the GEN:AgNPs at a concentration of 49 ±18 effectively restricted the growth of *P. aeruginosa* stains (Ridha *et al.,* 2024).Recent research has increasingly focused on the inhibitory efficacy of natural or synthetic substances on biofilm creation. Nosocomial pathogens like *S. aureus, P.aeruginosa,* and *P. mirabilis* are capable of causing various infections associated with biofilm formation (Shakibaie *et al.,* 2015). The half maximal inhibitory concentration IC50 of Amikacin: selenium nanoparticles was evaluated by determining their effect on the bioavailability of mature biofilm produced by PM4, PM5, PM7, and PM9. For all *P. mirabilis* samples, the IC_{50} values of AK and CS-SeNPs are higher than the IC_{50} values of AK: CS-SeNPs. As illustrated in Table 4, the conjugation of AK and CS-SeNPs at low concentrations resulted in a 50% reduction of the mature biofilm in the tested samples. The high concentration of AK at 1280 µg/mL caused the removal of 40% to 45% of mature biofilm *P. mirabilis* samples. As shown in (Fig. 5), the combination of AK: CS-SeNPs

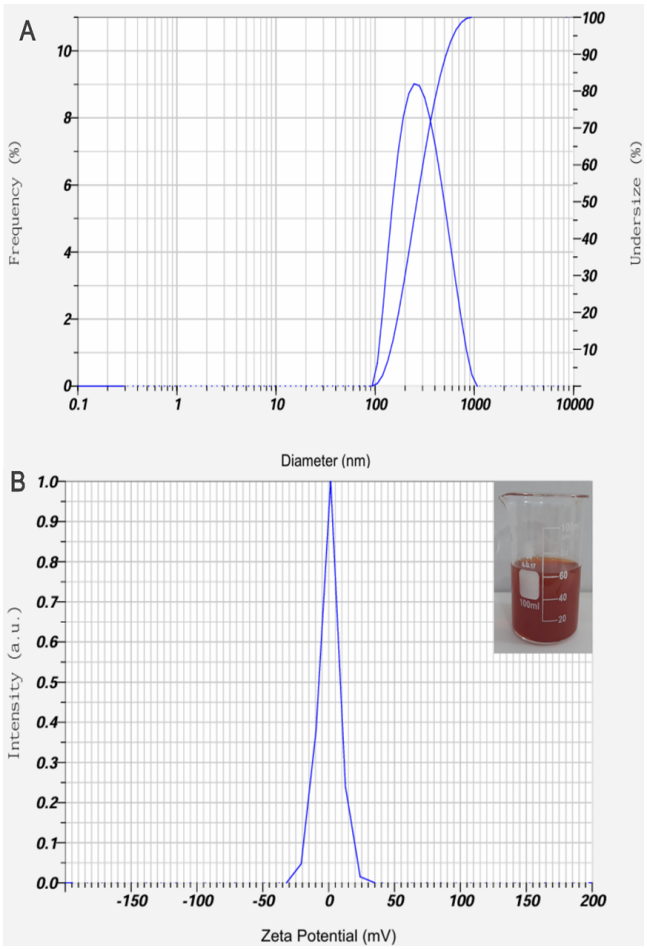

Fig. 4. *Characterization of selenium nanoparticles (CS-SeNPs) in liquid solution applying (A) DLS analysis indicating a hydro-diameter of CS-SeNPs was 302±151nm with a PDI of 0.188 , and (B) zeta potential spectra revealing that the surface charges of CS-SeNPs were equal to zero in spite of the stability of CS-SeNPs observed in the lateral image*

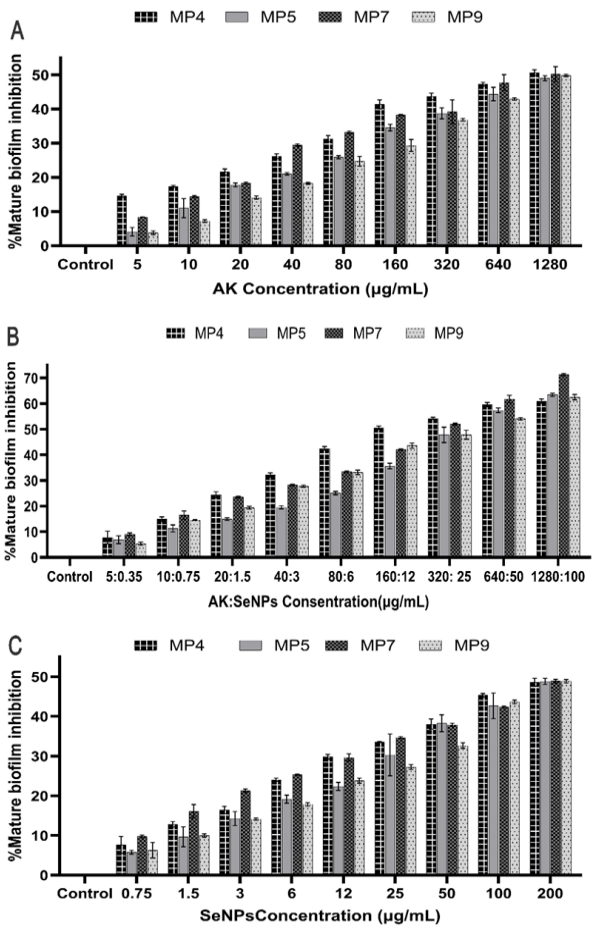

Fig.5. *Efficacy of AK, AK: CS-SeNPs, and CS-SeNPs on the mature biofilm of Proteus mirabilis samples at different concentrations*

reduces nearly the viability of 65% of mature biofilm for all *P.mirabilis* samples at 1280:100 µg/mL concentrations. Both PM4 and PM7 exposed to dual dilutions of AK:CS-SeNPs are more sensitive than PM5 PM6. The difference in the parentage of inhibition for the tested sample may be attributed to harbouring various contagious factors that assembled some samples that were more resistant to the treatment. The mature biofilms of *P.mirabilis* isolates treated with serial dilutions of SeNPs demonstrated a 45 %to 50 % reduction of the biofilm at 200 µg/mL. In Fig. 5, the mature biofilm biomass of PM4 and PM7 compared to PM5 and PM6 was diminished dramatically by raising CS-SeNP concentrations.

Conclusion

The increasing tolerance of microorganisms to different classes of antimicrobial agents poses a significant challenge, undermining their effectiveness against pathogens. Integrating conventional antibiotics with nanoparticles represents an innovative approach to augment the efficacy of classical antibiotics. SeNPs with a size of 68 ± 23 nm were successfully prepared and conjugated with amikacin. These nanoparticles have been implicated against *P.mirabilis* isolates. Chitosan-coated selenium nanoparticles enhanced the effect of amikacin against multidrug-resistant *P.mirabilis* isolates, reducing the bacterial growth of some isolates. AK:CS-SeNP conjugation inhibited the early stage of biofilm creation in *P. mirabilis* samples and reduced 60% of the viability of mature biofilm. The synergistic impact of AK:CS-SeNPs significantly reduces biofilm development compared to the application of both amikacin and stabilized chitosan selenium nanoparticles alone. The results indicate that the conjugation of AK:CS-SeNPs is a promising strategy targeting resistant *P. mirabilis* isolates.

ACKNOWLEDGEMENTS

The authors are grateful to the Microbiology Laboratory at the Science faculty at Babylon University, Iraq, for providing essential instruments for this study.

Conflict of interest

The authors declare that they have no conflict of interest.

REFERENCES

1. Al Jahdaly, B.A., Al-Radadi, N.S., Eldin, G.M.G., Almahri, A., Ahmed, M.K., Shoueir, K. & Janowska, I. (2021) . Selenium nanoparticles synthesized using an eco-friendly method: Dye decolorization from aqueous solutions, cell viability, antioxidant, and antibacterial effectiveness. *J. Mater. Res. Technol.* 11, 85–97. https://doi.org/10.1016/j.jmrt.2020.12.098
2. Bardbari, A.M., Arabestani, M.R., Karami, M., Keramat, F., Aghazadeh, H., Alikhani, M.Y. & Bagheri, K.P. (2018). Highly synergistic activity of melittin with imipenem and colistin in biofilm inhibition against multidrug-resistant strong biofilm producer strains of *Acinetobacter baumannii. Eur. J. Clin. Microbial. Infect. Dis*. 37, 443–454. https://doi.org/10.1007/s10096-018-3189-7
3. Bhattacharjee, S. (2016). DLS and zeta potential - What they are and what they are not? J. Control. Release 235, 337–351. https://doi.org/10.1016/j.jconrel.2016.06.017
4. Chen, W., Li, Y., Yang, S., Yue, L., Jiang, Q. & Xia, W. (2015). Synthesis and antioxidant properties of chitosan and carboxymethyl chitosan-stabilized selenium nanoparticles. *Carbohydr. Polym.* 132, 574–581. https://doi.org/10.1016/j.carbpol.2015.06.064
5. Fang, Ferric C. & R.T.S.(2020). Antimicrobial resistance—The glass Is half full. *N. Engl. J. Med*. 382, 1361–1363. https://doi.org/10.1056/nejme2002121
6. Geoffrion, L.D., Hesabizadeh, T., Medina-Cruz, D., Kusper, M., Taylor, P., Vernet-Crua, A., Chen, J., Ajo, A., Webster, T.J. & Guisbiers, G., (2020). Naked Selenium Nanoparticles for Antibacterial and Anticancer Treatments. *ACS Omega*. https://doi.org/10.1021/acsomega.9b03172
7. Haji, S.H., Ali, F.A., & Aka, S.T.H. (2022). Synergistic antibacterial activity of silver nanoparticles biosynthesized by carbapenem-resistant Gram-negative bacilli. *Sci. Rep*. 12, 1–13. https://doi.org/10.1038/s41598-022-19698-0
8. Huang, T., Holden, J.A., Heath, D.E., O'Brien-Simpson, N.M. & O'Connor, A.J. (2019). Engineering highly effective antimicrobial selenium nanoparticles through control of particle size. *Nanoscale* 11, 14937–14951. https://doi.org/10.1039/c9nr04424h
9. Huang, X., Chen, X., Chen, Q., Yu, Q., Sun, D. & Liu, J. (2016). Investigation of functional selenium nanoparticles as potent antimicrobial agents against superbugs. *Acta Biomater*. 30, 397–407. https://doi.org/10.1016/j.actbio.2015.10.041
10. Jacobsen, S.M., Stickler, D.J., Mobley, H.L.T. & Shirtliff, M.E. (2008). Complicated catheter-associated urinary tract infections due to Escherichia coli and *Proteus mirabilis. Clin. Microbial. Rev*. 21, 26–59. https://doi.org/10.1128/CMR.00019-07
11. Javed, R., Sajjad, A., Naz, S., Sajjad, H. & Ao, Q. (2022). Significance of Capping Agents of Colloidal Nanoparticles from the Perspective of Drug and Gene Delivery, Bioimaging, and Biosensing: An Insight. *Int. J. Mol. Sci.* 23. https://doi.org/10.3390/ijms231810521
12. Jernigan, J.A., Hatfield, K.M., Wolford, H., Nelson, R.E., Olubajo, B., Reddy, S.C., McCarthy, N., Paul, P., McDonald, L.C., Kallen, A., Fiore, A., Craig, M. & Baggs, J. (2020). Multidrug-Resistant Bacterial Infections in U.S. Hospitalized Patients, 2012–2017. *N. Engl. J. Med.* 382, 1309–1319. https://doi.org/10.1056/nejmoa1914433
13. Kaiser, T.D.L., Pereira, E.M., dos Santos, K.R.N., Maciel, E.L.N., Schuenck, R.P. &Nunes, A.P.F.(2013). Modification of the Congo red agar method to detect biofilm production by Staphylococcus epidermidis. *Diagn. Microbial. Infect. Dis*. 75, 235–239. https://doi.org/10.1016/j.diagmicrobio.2012.11.014
14. Kamer, A.M.A., El Maghraby, G.M., Shafik, M.M. & Al-Madboly, L.A. (2024). Silver nanoparticle with potential antimicrobial and antibiofilm efficiency against multiple drug resistant, extensive drug resistant *Pseudomonas aeruginosa* clinical isolates. BMC Microbial. 24, 1–16. https://doi.org/10.1186/s12866-024-03397-z
15. Karthik, K.K., Cheriyan, B.V., Rajeshkumar, S. & Gopalakrishnan, M. (2024). A review on selenium nanoparticles and their biomedical applications. *Biomed. Technol.* 6, 61–74. https://doi.org/10.1016/j.bmt.2023.12.001
16. Lin, W., Zhang, J., Xu, J.F. & Pi, J. (2021). The Advancing of Selenium Nanoparticles Against Infectious Diseases. *Front. Pharmacol*. 12, 1–16. https://doi.org/10.3389/fphar.2021.682284
17. Medina, Eva & D.H.P. (2016). " Tackling threats and future problems of multidrug-resistant bacteria. *Curr. Top. Microbiol. Immunol*. 33. https://doi.org/10.1007/82
18. Morones, J.R., Elechiguerra, J.L., Camacho, A., Holt, K., Kouri, J.B., Ramírez, J.T. &Yacaman, M.J. (2005). The bactericidal effect of silver nanoparticles. *Nanotechnology* 16, 2346–2353. https://doi.org/10.1088/0957-4484/16/10/059
19. Munir, M.U. & Ahmad, M.M. (2022). Nanomaterials Aiming to Tackle Antibiotic-Resistant Bacteria. *Pharmaceutics* 14, 1–17. https://doi.org/10.3390/pharmaceutics14030582
20. Pachouri, C., Tripathi, S., Shukla, S. & Pandey, A. (2021). Development and Evaluation of Chitosan Nanoparticles Based Dry Powder Inhalation Formulations of Isoniazid and Its Release Kinetics. Oxid. Commun. 44, 755–768.
21. Ridha, D.M., AL-Rafyai, H.M. & Najii, N.S. (2021). Bactericidal Potency of Green Synthesized Silver Nanoparticles against Waterborne *Escherichia coli* Isolates. *Nano Biomed. Eng*. 13, 372–379. https://doi.org/10.5101/nbe.v13i4.p372-379
22. Ridha, D.M., AL-Rafyai, H.M. & Saleh, M.A.A.-J.M. (2024). Evaluation of the Antibacterial Impact of the Conjugated Gentamycin-biosynthesized Silver Nanoparticles on Resistant *Pseudomonas aeruginosa* Isolates *In Vitro. Nano Biomed*. Eng. 0–10. https://doi.org/10.26599/nbe.2024.9290067
23. Roy, N., Nivedya, T., Paira, P. & Chakrabarty, R. (2025). Selenium-based nanomaterials: Green and conventional synthesis methods, applications, and advances in dye degradation. RSC Adv. 15, 3008–3025. https://doi.org/10.1039/d4ra07604d
24. San Keskin, N.O., Akbal Vural, O. & Abaci, S. (2020). Biosynthesis of Noble Selenium Nanoparticles from Lysinibacillus sp. NOSK for Antimicrobial, Antibiofilm Activity, and Biocompatibility. *Geomicrobiol. J.* 37, 919–928. https://doi.org/10.1080/01490451.2020.1799264

25. Schaffer, J.N. & Pearson, M.M. (2016). Proteus mirabilis and urinary tract infections. Urin. Tract Infect. Mol. Pathog. *Clin. Manag*. 383–433. https://doi.org/10.1128/9781555817404.ch17
26. Sentkowska, A. & Pyrzyńska, K. (2022). The Influence of Synthesis Conditions on the Antioxidant Activity of Selenium Nanoparticles. *Molecules* 27, 1–14. https://doi.org/10.3390/molecules27082486
27. Shahmoradi, S., Shariati, A., Zargar, N., Yadegari, Z., Asnaashari, M., Amini, S.M. & Darban-Sarokhalil, D. (2021). Antimicrobial effects of selenium nanoparticles in combination with photodynamic therapy against Enterococcus faecalis biofilm. Photodiagnosis *Photodyn. Ther*. 35, 102398. https://doi.org/10.1016/j.pdpdt.2021.102398
28. Shakibaie, M., Forootanfar, H., Golkari, Y., Mohammadi-Khorsand, T. & Shakibaie, M.R. (2015). Anti-biofilm activity of biogenic selenium nanoparticles and selenium dioxide against clinical isolates of Staphylococcus aureus, Pseudomonas aeruginosa, and Proteus mirabilis. *J. Trace Elem. Med. Biol*. 29, 235–241. https://doi.org/10.1016/j.jtemb.2014.07.020
29. Sharma, D., Maheshwari, D., Philip, G., Rana, R., Bhatia, S., Singh, M., Gabrani, R., Sharma, S.K., Ali, J., Sharma, R.K. & Dang, S. (2014). Formulation and optimization of polymeric nanoparticles for intranasal delivery of lorazepam using Box-Behnken design: In vitro and *in vivo* evaluation. Biomed Res. Int. 2014. https://doi.org/10.1155/2014/156010
30. 31. Tumbarello, M., Trecarichi, E.M., Fiori, B., Losito, A.R., D'Inzeo, T., Campana, L., Ruggeri, A., Di Meco, E., Liberto, E., Fadda, G., Cauda, R. & Spanu, T. (2012). Multidrug-resistant Proteus mirabilis bloodstream infections: Risk factors and outcomes. Antimicrob. *Agents Chemother.* 56, 3224–3231. https://doi.org/10.1128/AAC.05966-11
31. Wadhwani, S.A., Gorain, M., Banerjee, P., Shedbalkar, U.U., Singh, R., Kundu, G.C. & Chopade, B.A. (2017). Green synthesis of selenium nanoparticles using Acinetobacter sp. SW30: Optimization, characterization and its anticancer activity in breast cancer cells. *Int. J. Nanomedicine* 12, 6841–6855. https://doi.org/10.2147/IJN.S139212
32. 33. WHO. (2017). GLASS | Global antimicrobial resistance surveillance system (GLASS) report 2016-17, Who.
33. Yuan, Q., Xiao, R., Afolabi, M., Bomma, M. & Xiao, Z. (2023). Evaluation of Antibacterial Activity of Selenium Nanoparticles against Food-Borne Pathogens. *Microorganisms* 11. https://doi.org/10.3390/microorganisms11061519
34. Zhang, C., Zhai, X., Zhao, G., Ren, F. & Leng, X. (2015). Synthesis, characterization, and controlled release of selenium nanoparticles stabilized by chitosan of different molecular weights. Carbohydr. *Polym.* 134, 158–166. https://doi.org/10.1016/j.carbpol.2015.07.065
35. Zhang, H., Li, Z., Dai, C., Wang, P., Fan, S., Yu, B. & Qu, Y. (2021). Antibacterial properties and mechanism of selenium nanoparticles synthesized by *Providencia* sp. DCX. *Environ. Res.* 194, 110630. https://doi.org/10.1016/j.envres.2020.110630
36. Zou, L., Wang, J., Gao, Y., Ren, X., Rottenberg, M.E., Lu, J. & Holmgren, A. (2018). Synergistic antibacterial activity of silver with antibiotics correlating with the upregulation of the ROS production. *Sci. Rep*. 8, 1–11. https://doi.org/10.1038/s41598-018-29313-w